Phase diagram of the Anderson-Falicov-Kimball model at half filling

M. A. Gusmão
Instituto de Física, Universidade Federal do Rio Grande do Sul, CP 15051, 91501-970 Porto Alegre, Brazil
(Received 14 January 2008; revised manuscript received 23 May 2008; published 16 June 2008)

We study the Falicov-Kimball model [Phys. Rev. Lett. **22**, 997 (1969)] at half-filling in the presence of on-site disorder. Using dynamical mean-field theory, we evaluate densities of states appropriately averaged over a continuous distribution of local energies, identifying the phases that appear upon varying the Coulomb interaction and disorder strength. We focus on the existence and stability of the chessboard ordered state, including it in the complete phase diagram.

DOI: 10.1103/PhysRevB.77.245116 PACS number(s): 71.10.Fd, 71.23.−k, 71.30.+h, 75.10.−b

I. INTRODUCTION

The interplay between strong correlation and disorder in narrow-band electronic systems is of great interest, as the band filling is experimentally controlled through doping, which naturally introduces some amount of disorder. Among the most cited examples are high-T_c cuprates[1] such as $La_{1-x}Sr_xCuO_4$, in which the random substitution of Sr for La ions provides a randomly varying potential acting on the correlated holes of CuO_2 planes.

Viewed independently, both electronic correlations and disorder are known to drive metal-insulator transitions (MITs), although they are of different nature. Coulomb correlations tend to open a gap in the single-particle excitation spectrum, mainly for a nearly half-filled band, reflecting the fact that electrons with opposite spins avoid occupying the same lattice site. The opening of this correlation gap characterizes what is known as the Mott-MIT.[2] On the other hand, disorder-induced deviations from a periodic potential provide strong scattering of individual electrons, eventually yielding localization of the electronic states at the Fermi level. This is usually referred to as *Anderson localization* after the pioneer work by Anderson.[3] The interplay between these two scenarios in systems that are both correlated and disordered has attracted a great deal of attention[4] but still constitutes a big challenge, especially in what concerns a comprehensive theoretical description.

The prototype model for this problem utilizes the Hubbard Hamiltonian with a random distribution of on-site energies, often called Anderson-Hubbard model. For more than a decade, dynamical mean-field theory (DMFT) has been one of the most accepted nonperturbative frameworks to deal with models of strongly correlated systems.[5] However, simply incorporating disorder effects into this approach through an *arithmetic* average of the local density of states (DOS) does not yield Anderson localization in the sense that the DOS remains finite at the Fermi level (in the absence of correlations) for arbitrary disorder strength. Recently,[6] DMFT was appropriately extended through the realization that a *geometrically* averaged DOS provides a good approximation for the most probable (or *typical*) DOS, vanishing when the states are localized.

The most difficult task within DMFT is to solve the single-site (or impurity) problem to which the lattice problem is mapped. Although this mapping is exact in infinite dimensions, the resulting impurity problem is far from trivial, and one needs to resort to approximations, such as the numerical renormalization group (NRG).[7] Within this general scheme (DMFT+NRG+typical DOS), a detailed study of the Anderson-Hubbard model in the nonmagnetic case was reported by Byczuk *et al.*[8] However, it is extremely interesting to take magnetic ordering into account since it is well known that the paramagnetic (PM) state of the half-filled Hubbard model (in the absence of disorder) is unstable against antiferromagnetic (AF) ordering, at least for bipartite lattices. Although a study of this problem including magnetic order has been reported earlier,[9] its results have not been connected with the PM phase diagram of Ref. 8.

Given that including magnetism enhances the technical difficulties to solve the problem, we will focus our attention on the Falicov-Kimball (FK) model[10] or Anderson-Falicov-Kimball in the presence of disorder, which can be viewed as a "simplified version"[11] of the Hubbard model in which hopping processes are suppressed for electrons of a given spin orientation. The FK model is especially interesting because it is exactly solvable in infinite dimensions.[12–16] Besides, it contains important aspects of strong-correlation physics, including the Mott-MIT, and a kind of AF ordering in which the nonmoving electrons occupy alternate sites on the lattice (chessboard pattern), while the moving ones tend to occupy preferably the remaining sites. This gives rise to a staggered spin distribution when viewed as a simplified Hubbard model and mimics an AF phase.

Recently, the FK model with disorder was studied by Byczuk[17] for the homogeneous case. Our main goal here is to add to the knowledge obtained from previous studies[8,17] by including the chessboard ordering, thus constructing a more complete phase diagram in terms of Coulomb interaction and disorder strength.

II. MODEL AND DMFT APPROACH

We write down the model Hamiltonian as

$$H = \sum_i \varepsilon_i (n_i^c + n_i^f) - t \sum_{\langle ij \rangle} c_i^\dagger c_j + U \sum_i n_i^c n_i^f, \qquad (1)$$

where ε_i is a random on-site energy, t is the hopping integral of the moving (c) spinless fermions, and U stands for the local Coulomb interaction between the two kinds of fermions, c and f. The usual notation has been employed for fer-

mion creation, annihilation, and number operators in the Wannier representation. We will restrict our analysis to a half-filled system, i.e., with $\Sigma_i n_i^c = \Sigma_i n_i^f = N/2$, with N being the total number of lattice sites. In order to keep a connection with the Hubbard model, we choose the same local energies for both c and f particles. In the nonrandom case, a local energy $\varepsilon = -U/2$ is consistent with a fixed chemical potential $\mu = 0$ at half-filling. Keeping this chemical potential, we then choose a uniform distribution of random energies $P(\varepsilon_i)$, of width Δ, and centered at $-U/2$.

III. HOMOGENEOUS CASE

Within DMFT,[5] the lattice is replaced by a single site with a dynamical mean field that takes electrons in and out of this site. For the FK model, this dynamical mean field acts only on the moving fermions. The lattice self-energy is purely local, and a self-consistency condition is obtained by equating the effective single-site Green's function (GF) and the site-diagonal one for the lattice. In the disordered case, this self-consistency only makes sense for averaged Green's functions, for which translational invariance is restored. It assumes the form

$$G_{ii}^{\mathrm{av}}(\omega_n) = \int \frac{\rho_0(\varepsilon)d\varepsilon}{[G_{ii}^{\mathrm{av}}(\omega_n)]^{-1} + \lambda(\omega_n) - \varepsilon}, \tag{2}$$

where $\lambda(\omega_n)$ denotes a Fourier component of the above mentioned mean field and $\rho_0(\varepsilon)$ is the DOS for the uncorrelated band. Here we use a semielliptical DOS, corresponding to a Bethe lattice of infinite coordination number. We choose $\rho_0(\varepsilon) = (2/\pi)\sqrt{1-\varepsilon^2}$, so that the half-width of the bare band defines our energy unit.

In order to obtain a self-consistent solution, one needs to explicitly solve the effective single-site problem. As we mentioned before, an exact solution exists in the case of the FK model,[12] so that we can write an explicit expression for the local GF,

$$G_{ii}(\omega_n) = \frac{1 - \langle n^f \rangle}{i\omega_n - \varepsilon_i - \lambda(\omega_n)} + \frac{\langle n^f \rangle}{i\omega_n - \varepsilon_i - U - \lambda(\omega_n)}. \tag{3}$$

Notice that this GF depends not only on an explicit realization of the random site energies but also on the global self-consistent quantities $\lambda(\omega_n)$ and $\langle n^f \rangle$, the latter being the average number of f fermions per site. We first focus on the homogeneous solution at half-filling, for which the average occupation is 1/2 for both kinds of particles. We will discuss the calculation of nontrivial number averages later on when we address the ordered state. Equations (2) and (3) are written for Matsubara (or finite-temperature) Green's functions. The corresponding retarded versions are obtained through the usual analytical continuation $i\omega_n \to \omega + i0^+$, which is needed to obtain the local DOS from the imaginary part of the retarded GF.

Arithmetic averaging can be directly performed on Eq. (3), after analytical continuation to real frequencies, with the imaginary part of the resulting GF yielding the arithmetically averaged DOS $\rho_a(\omega)$. On the other hand, the geometrical average is more involved: we must calculate $\rho_i(\omega) = -\mathrm{Im}\, G_{ii\uparrow}(\omega)/\pi$, evaluate its geometrical average $\rho_g(\omega) = \exp[\ln \rho(\omega)]_a$, and then obtain its Hilbert transform $\mathrm{Re}\, G_g(\omega) = \int d\omega' \rho_g(\omega')/(\omega - \omega')$ in order to build up the full geometrically averaged GF to be used in the self-consistency condition [Eq. (2)]. In our notation $[\cdots]_a$ denotes arithmetic average over the random energies.

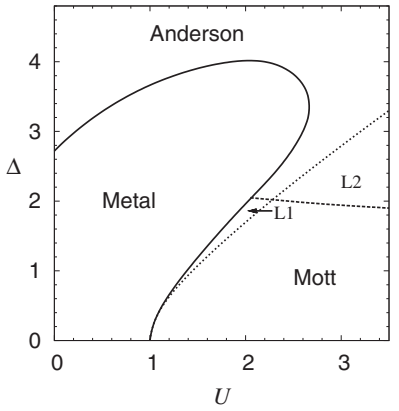

FIG. 1. Phase diagram of the half-filled AFK model in the homogeneous case showing a metallic phase and two insulating regimes, Mott and Anderson. Two special regions are indicated: L1—localized states inside the Mott gap; L2—true Mott gap, but no extended states.

We will not discuss the details of the DOS for different values of U and Δ obtained with both kinds of average, as it has been extensively done in Ref. 17. Before addressing the ordered case, we just want to mention that five different situations exist in the homogeneous solution, characterized by different combinations of values of ρ_a and ρ_g:

(1) $\rho_a(0) \neq 0$, $\rho_g(0) \neq 0$: metal;
(2) $\rho_a(0) = 0$, $\rho_g(0) = 0$, $\int \rho_g(\omega) d\omega \neq 0$: Mott insulator;
(3) $\rho_a(0) \neq 0$, $\rho_g(0) = 0$, $\int \rho_g(\omega) d\omega \neq 0$: localized states inside the Mott gap;
(4) $\rho_a(0) = 0$, $\int \rho_g(\omega) d\omega = 0$: Anderson localization with a Mott gap; and
(5) $\rho_a(0) \neq 0$, $\int \rho_g(\omega) d\omega = 0$: Anderson localization without a Mott gap.

These regimes appear for appropriate values of U and Δ and define the various regions of the phase diagram shown in Fig. 1. Roughly speaking, a metallic state exists for small U and Δ, Mott insulator is the stable state for large U and small Δ, while large enough Δ gives rise to Anderson localization.

IV. CHESSBOARD ORDERING

We now turn to the chessboard ordered case. First of all, we divide the lattice into two sublattices, A ("black") and B ("white"), which are related to the condition $\langle n^f \rangle_A = 1 - \langle n^f \rangle_B$. The order parameter may be defined as $\Delta n^f \equiv \langle n^f \rangle_A - 1/2$.

In the ordered state, the local GF for c electrons [Eq. (3)] keeps its form except for the inclusion of A or B subscripts depending on the sublattice to which the site belongs. The self-consistency condition [Eq. (2)] now reads[5]

$$G_{ii\alpha}^{\mathrm{av}}(\omega_n) = \frac{\xi}{\xi_\alpha} \int \frac{\rho_0(\varepsilon)}{\xi - \varepsilon} d\varepsilon, \tag{4}$$

where $\alpha = A, B$ and

$$\xi_\alpha \equiv [G^{\mathrm{av}}_{ii\alpha}(\omega_n)]^{-1} + \lambda_\alpha(\omega_n), \quad \xi \equiv \sqrt{\xi_A \xi_B}. \tag{5}$$

In this context, we use arithmetic average, since all states (not only the extended ones) contribute to the site occupation.

In contrast to the homogeneous case, average occupation numbers for both fermion species must be evaluated self-consistently, as they are no longer fixed at 1/2. While $\langle n^c \rangle$ is obtained by summing the average GF over frequencies, evaluation of $\langle n^f \rangle$ is more involved since there is no GF associated to these particles in the FK model. This would not be the case for the Hubbard model when both averages could be treated on equal footing at the price of losing the exact solution. Following early works on the FK model,[12,15] we write down an expression for $\langle n_i^f \rangle$ obtained by deriving the GF [Eq. (3)] from the exact partition function. It can be expressed[14] as a Fermi function,

$$\langle n_i^f \rangle = \frac{1}{e^{\beta E_i^f} + 1}, \tag{6}$$

where $\beta \equiv 1/T$ (the Boltzmann constant is taken as $k_B = 1$) and E_i^f can be viewed as an effective f-fermion energy, defined by

$$E_i^f \equiv \varepsilon_i + T \sum_n [\ln(i\omega_n - \varepsilon_i - \lambda_n) - \ln(i\omega_n - \varepsilon_i - U - \lambda_n)] e^{i\omega_n 0+}, \tag{7}$$

with the shorthand notation $\lambda_n \equiv \lambda(\omega_n)$. Notice that the first term in the right-hand side is usually[13,14] written as E_f (or some similar notation) because it comes from the local energy of the f particles. Here, as we mentioned above, it is chosen as locally equal to the c-particle energies ε_i in order to ensure the half-filling condition. Furthermore, we use the same expressions obtained for the nonrandom case, just adding the site label, as those expressions refer to a single effective site.

We see now that the global $\langle n^f \rangle$ of Eq. (3) is obtained here as a local quantity, so that we must choose a consistent way of averaging it over disorder. Given that $\langle n^c \rangle$, as obtained from the averaged GF, can be viewed as $[\langle n_i^c \rangle]_a$, we can also obtain the average f-particle occupation as $\langle n^f \rangle = [\langle n_i^f \rangle]_a$, averaging Eq. (6) over disorder. Obviously, this has to be done for each sublattice, even though, for economy of notation, we omitted the sublattice index in the above discussion about occupation numbers.

Before describing our numerical results, it is important to look at a technical aspect of the calculation in some detail. The sums of logarithms that appear in Eq. (7) have to be handled with care, as their convergence is not trivial. We rewrite that equation as

$$E_i^f = E_i^{f(\mathrm{at})} + T \sum_n [\Delta L_n(\varepsilon_i) - \Delta L_n(\varepsilon_i + U)] e^{i\omega_n 0+}, \tag{8}$$

where $E_i^{f(\mathrm{at})}$ stands for the atomic limit of E_i^f, $L_n(x) \equiv \ln(i\omega_n - x - \lambda_n)$, and $\Delta L_n(x)$ denotes the deviation of $L_n(x)$ from its value at the atomic limit, i.e., calculated with $\lambda_n = 0$. The sums over Matsubara frequencies are now quickly convergent as $\lambda_n \to 0$ for large ω_n. On the other hand, the corresponding sums in $E_i^{f(\mathrm{at})}$ can be evaluated analytically by transforming them into integrals over the complex-frequency plane.[16] The result is

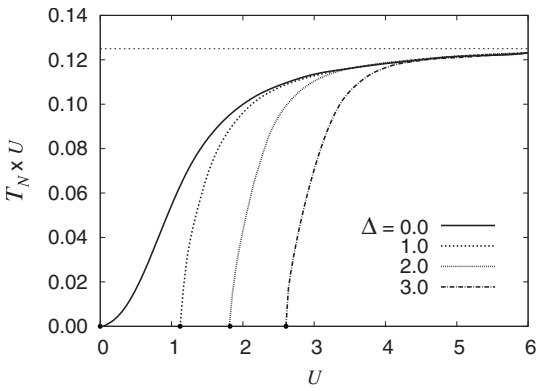

FIG. 2. Variation of the critical temperature T_N of the chessboard phase as a function of U for different values of the disorder parameter Δ. The top horizontal line corresponds to the Ising limit, $T_N = 1/8U$.

$$\exp(\beta E_i^{f(\mathrm{at})}) = \frac{1 + e^{\beta \varepsilon_i}}{1 + e^{-\beta(\varepsilon_i + U)}}. \tag{9}$$

Notice that in the nonrandom atomic limit, when $\varepsilon_i = -U/2$, Eqs. (6) and (9) yield $n_i^{f(\mathrm{at})} = 1/2$, as expected.

Starting with a nonzero Δn^f and numerically solving our set of self-consistent equations, we find that a chessboard ordered solution exists for any nonzero U, as in the clean case.[12] This solution is stable below a critical temperature that we will call *Néel temperature*, T_N, due to the previously mentioned analogy with AF order in the Hubbard model. The effect of disorder is to reduce T_N, which vanishes at a critical Δ above which the chessboard solution no longer exists. For fixed Δ, reduction in the critical temperature is more pronounced for small U, but T_N tends to its clean-limit value as U increases. This is shown in Fig. 2 for some values of Δ. We chose to plot $T_N \times U$ vs U to stress the fact that all curves approach the large-U localized-spin limit, where the Hubbard (FK) model maps into a Heisenberg (Ising) model with an exchange constant proportional to t^2/U. All curves coincide in this limit, as the effective exchange constant is independent of disorder. Similar results (plotted as T_N vs U) where reported for the Hubbard model in Ref. 9.

From the results just discussed, it is clear that a phase diagram for the homogeneous case is meaningless in the low-Δ/large-U region, where the chessboard solution is stable. Collecting the critical disorder strengths for each U, we construct a "magnetic" phase diagram $\Delta \times U$ that we superpose on the homogeneous one, obtaining the complete phase diagram of the model, shown in Fig. 3. Except for the Anderson-localization regime and the metallic state, all the other features of the homogeneous phase diagram (Fig. 1) are "buried" inside the chessboard phase, including the Mott-MIT point at $U = 1, \Delta = 0$.

V. CONCLUSIONS

The important information contained in Fig. 3 is that the chessboard phase dominates at "weak" disorder. Keeping the

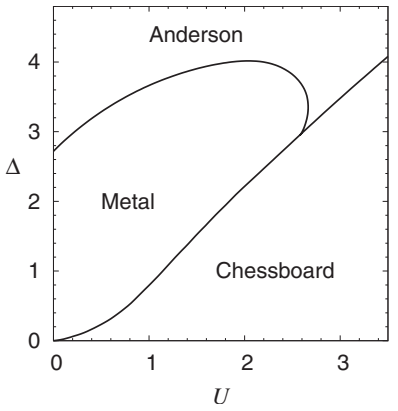

FIG. 3. Complete phase diagram of the half-filled AFK model, including all the thermodynamically stable phases in the limit $T \to 0$.

analogy, we can expect AF ordering to dominate the low-disorder region for the Hubbard model. This fact casts doubts about any analysis of the Mott-MIT that does not take magnetic ordering into account. Notice that at the critical U for the Mott transition at zero Δ (in our units, $U=1$) the chessboard phase is stable up to $\Delta \sim U$. This is nearly half the bandwidth or approximately the Fermi energy. Such a huge disorder strength is quite unrealistic.

It may be argued that the chessboard phase becomes unstable for disorder strengths that are substantially smaller than those that yield Anderson localization, at least for Coulomb interactions not much above the Mott-MIT point. However, one may interpret that it is actually the critical disorder for Anderson localization that is extremely high (about four times the Fermi energy), which is probably due to the large spatial dimensionality implied by DMFT.

In summary, we have constructed a complete phase diagram of the Anderson-Falicov-Kimball model at half-filling, allowing for the presence of chessboard ordering. The metallic phase as well as the Anderson-insulator state obtained in the homogeneous solution are still present at intermediate and strong disorder, but the strong-correlation region ($U > \Delta$) is dominated by the chessboard phase. Taking also into account the quantitative information about temperature effects, our results set important reference points for an old discussion in the field of strongly correlated systems: whether studies of the Mott-MIT neglecting magnetic ordering are meaningful or not. It is clear that further progress is needed in this field, mainly with respect to the inclusion of band-filling effects, as well as exploring other models of correlated electrons.

ACKNOWLEDGMENT

We acknowledge support from Conselho Nacional de Desenvolvimento Científico e Tecnológico (CNPq), Brazil.

[1] M. Imada, A. Fujimori, and Y. Tokura, Rev. Mod. Phys. **70**, 1039 (1998).
[2] N. F. Mott, Proc. Phys. Soc., London, Sect. A **62**, 416 (1949); *Metal-Insulator Transitions*, 2nd ed. (Taylor & Francis, London, 1990).
[3] P. W. Anderson, Phys. Rev. **109**, 1492 (1958).
[4] P. A. Lee and T. V. Ramakrishnan, Rev. Mod. Phys. **57**, 287 (1985); D. Belitz and T. R. Kirkpatrick, *ibid.* **66**, 261 (1994); H. von Löhneysen, Adv. Solid State Phys. **40**, 143 (2000); S. V. Kravchenko and M. P. Sarachik, Rep. Prog. Phys. **67**, 1 (2004).
[5] A. Georges, G. Kotliar, W. Krauth, and M. J. Rozenberg, Rev. Mod. Phys. **68**, 13 (1996).
[6] V. Dobrosavljević, A. A. Pastor, and B. K. Nikolić, Europhys. Lett. **62**, 76 (2003).
[7] K. G. Wilson, Rev. Mod. Phys. **47**, 773 (1975); R. Bulla, Phys. Rev. Lett. **83**, 136 (1999); W. Hofstetter, *ibid.* **85**, 1508 (2000).
[8] K. Byczuk, W. Hofstetter, and D. Vollhardt, Phys. Rev. Lett. **94**, 056404 (2005).
[9] M. Ulmke, V. Janiš, and D. Vollhardt, Phys. Rev. B **51**, 10411 (1995).
[10] L. M. Falicov and J. C. Kimball, Phys. Rev. Lett. **22**, 997 (1969).
[11] P. G. J. van Dongen and D. Vollhardt, Phys. Rev. Lett. **65**, 1663 (1990).
[12] U. Brandt and C. Mielsch, Z. Phys. B: Condens. Matter **75**, 365 (1989); U. Brandt and C. Mielsch, *ibid.* **79**, 295 (1990); U. Brandt and C. Mielsch, *ibid.* **82**, 37 (1991).
[13] V. Janiš, Z. Phys. B: Condens. Matter **83**, 227 (1991).
[14] Q. Si, G. Kotliar, and A. Georges, Phys. Rev. B **46**, 1261 (1992).
[15] J. K. Freericks and V. Zlatić, Rev. Mod. Phys. **75**, 1333 (2003).
[16] A. M. Shvaika and J. K. Freericks, Phys. Rev. B **67**, 153103 (2003).
[17] K. Byczuk, Phys. Rev. B **71**, 205105 (2005).